

## Selective area atomic layer deposition of rhodium and effective work function characterization in capacitor structures

K. J. Park and G. N. Parsons

Citation: [Applied Physics Letters](#) **89**, 043111 (2006); doi: 10.1063/1.2234846

View online: <http://dx.doi.org/10.1063/1.2234846>

View Table of Contents: <http://scitation.aip.org/content/aip/journal/apl/89/4?ver=pdfcov>

Published by the [AIP Publishing](#)

---

### Articles you may be interested in

[Degradation analysis and characterization of multifilamentary conduction patterns in high-field stressed atomic-layer-deposited TiO<sub>2</sub>/Al<sub>2</sub>O<sub>3</sub> nanolaminates on GaAs](#)

*J. Appl. Phys.* **112**, 064113 (2012); 10.1063/1.4754510

[Structural and electrical properties of atomic layer deposited Al-doped ZrO<sub>2</sub> films and of the interface with TaN electrode](#)

*J. Appl. Phys.* **112**, 014107 (2012); 10.1063/1.4731746

[Atomic layer deposition of Ru onto organic monolayers: Shifting metal effective work function using monolayer structure](#)

*J. Vac. Sci. Technol. A* **30**, 01A162 (2012); 10.1116/1.3671938

[Atomic layer deposited TaC y metal gates: Impact on microstructure, electrical properties, and work function on HfO<sub>2</sub> high- \$k\$  dielectrics](#)

*J. Appl. Phys.* **102**, 104509 (2007); 10.1063/1.2817620

[Effective work function modification of atomic-layer-deposited-TaN film by capping layer](#)

*Appl. Phys. Lett.* **89**, 032113 (2006); 10.1063/1.2234288

---

An advertisement for COMSOL Multiphysics simulation projects. The background is dark with a grid pattern. On the left, there is a 3D cutaway view of a mechanical part with a red and yellow color gradient. The text 'Over 600 Multiphysics Simulation Projects' is prominently displayed in white and blue. A blue button with white text says 'VIEW NOW >>'. The COMSOL logo is in the bottom right corner.

Over 600 Multiphysics Simulation Projects

[VIEW NOW >>](#)

COMSOL

## Selective area atomic layer deposition of rhodium and effective work function characterization in capacitor structures

K. J. Park<sup>a)</sup> and G. N. Parsons

Department of Chemical and Biomolecular Engineering, North Carolina State University, Raleigh, North Carolina 27695

(Received 23 January 2006; accepted 4 June 2006; published online 26 July 2006)

Atomic layer deposition (ALD) of rhodium was investigated using rhodium(III) acetylacetonate and oxygen, and capacitance versus voltage is used to extract the effective work function in metal/insulator/semiconductor structures. Self-limiting growth was observed, and the resistivity of Rh deposited at 300 °C is  $\sim 10 \mu\Omega \text{ cm}$ , approximately a factor of 2 larger than the Rh bulk resistivity ( $4.3 \mu\Omega \text{ cm}$ ). Selective area deposition is achieved using patterned resist layers, enabling capacitor fabrication without Rh etching. In the as-deposited state, the effective work function was measured to be 5.43 and 5.25 eV on  $\text{SiO}_2$  and  $\text{HfO}_2$  dielectrics, respectively. The ALD Rh films formed under conditions used likely contain residual oxygen which can affect oxygen vacancy creation and the effective work function at the metal/dielectric interface. © 2006 American Institute of Physics. [DOI: 10.1063/1.2234846]

Metals are of interest for advanced metal/oxide/semiconductor (MOS) devices to replace polycrystalline silicon gate electrodes to avoid effects of charge depletion<sup>1</sup> and to serve as nucleation and barrier layers for copper interconnects.<sup>2</sup> Noble metals, in particular, Ru, Rh, Pd, Re, Ir, and Pt, are of interest for positive channel MOS (PMOS) gate electrodes because their vacuum work function is near the conduction band edge of silicon. The effective work function ( $\Phi_{m,\text{eff}}$ ) of Ru in a MOS structure has been measured<sup>3-5</sup> to be 4.7–5.2 eV, but materials with higher  $\Phi_{m,\text{eff}}$  are desired. In addition, the value of  $\Phi_{m,\text{eff}}$  on high- $k$  dielectrics is generally somewhat lower than that on  $\text{SiO}_2$ ,<sup>6,7</sup> and the effective work function of PMOS gates can be sensitive to oxygen vacancy generation at the metal/high- $k$  interface.<sup>8,9</sup> Atomic layer deposition (ALD) has been used to deposit many noble metals,<sup>2,3,10-13</sup> but the effective work function of ALD noble metals is not widely reported.<sup>3,13</sup> This letter presents results of thermal ALD of rhodium deposited using rhodium(III) acetylacetonate [ $\text{Rh}(\text{acac})_3$ ] and oxygen, and deposition results are generally consistent with the work of Aaltonen *et al.*<sup>12</sup> that shows ALD-type growth using these precursors. Selective area deposition of Rh is demonstrated using patterned photoresist, and the effective work function of selectively deposited ALD Rh is characterized on  $\text{HfO}_2$  and  $\text{SiO}_2$  dielectrics using capacitance analysis.

Atomic layer deposition was carried out in a homebuilt hot-wall quartz tube reactor with a base pressure of  $\sim 5 \times 10^{-6}$  Torr. The  $\text{Rh}(\text{acac})_3$  precursor is a solid at room temperature, but attains a vapor pressure of  $\sim 20$  mTorr upon heating to 150 °C. The reactor was purged with Ar at an operating pressure of 0.9 Torr, and the precursor and oxidant gases were introduced into the reactor in pulses of 15 and 10 s, respectively, with a 15 s Ar purge between each reactant. The  $\text{Rh}(\text{acac})_3$  was carried into the reactor using Ar flow, and the total gas flow rate was constant at 300 SCCM (SCCM denotes cubic centimeter per minute at STP). Substrates were chemical vapor deposited  $\text{HfO}_2$  and thermally grown  $\text{SiO}_2$ . Surface profilometry was used to measure film

thickness, and x-ray photoelectron spectroscopy (XPS) and Auger electron spectroscopy (AES) were used to determine the film composition and nucleation selectivity. The film resistivity was measured with a four-point probe, and capacitance versus voltage ( $CV$ ) was measured using an HP 4284A LCR meter at 1 MHz using  $p$ -type silicon substrates with doping levels of  $7 \times 10^{17}$  and  $3 \times 10^{15} \text{ cm}^{-3}$  for  $\text{SiO}_2$  and  $\text{HfO}_2$ , respectively. For some samples, post-metallization-annealing (PMA) was done under a forming gas (10:1  $\text{N}_2:\text{H}_2$ ) at 400 °C for 30 min.

The Rh film thickness per deposition cycle is plotted versus deposition temperature (on  $\text{HfO}_2$  substrates) in Fig. 1. Under these conditions, a deposition rate between 0.9 and 1.2 Å/cycle is observed between  $\sim 275$  and 310 °C. At 300 °C, saturation in growth/cycle is observed between 0.9 and 1.2 Å/cycle, which is somewhat larger than  $\sim 0.8$  Å/cycle obtained by Aaltonen *et al.*<sup>12</sup> Recent results in our laboratory suggest that for ALD of noble metals deposited by the ligand oxidation process,<sup>10,12</sup> the amount of metal deposition per cycle scales with the extent of oxygen exposure/cycle, so differences in pressure or cycle time can affect metal growth rate per cycle, even under self-limiting ALD conditions.<sup>14</sup> Figure 1 also shows that Rh film resistivity decreases with increasing temperature and reaches a minimum of  $10 \mu\Omega \text{ cm}$  at 300 °C, approximately a factor of 2

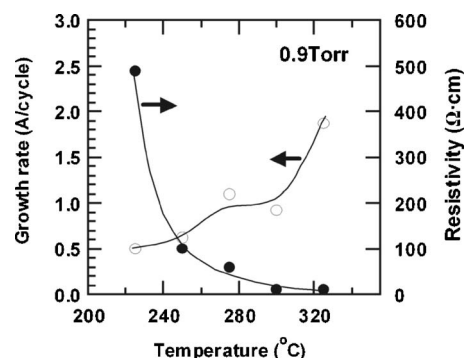


FIG. 1. ALD rhodium film growth rate and resistivity vs deposition temperature as deposited on chemical vapor deposited (CVD)  $\text{HfO}_2$  substrate.

<sup>a)</sup>Electronic mail: kpark@ncsu.edu

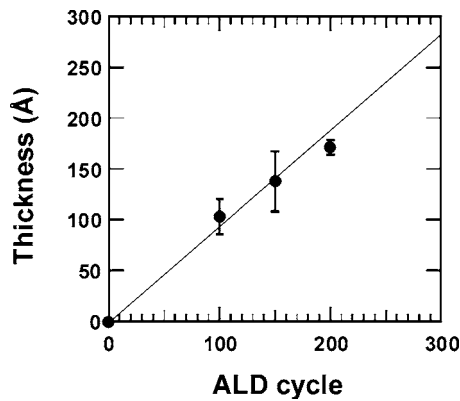


FIG. 2. Rhodium film thickness vs number of ALD cycles deposited on  $\text{HfO}_2$ .

larger than the Rh bulk resistivity of  $4.3 \mu\Omega \text{ cm}$ . At  $300^\circ \text{C}$  the thickness per cycle increases linearly as shown in Fig. 2, consistent with a typical ALD process. The error bars represent  $\pm 1$  standard deviation obtained from approximately four to six measurements for each sample.

The XPS spectra of rhodium films deposited on silicon oxide are shown in Fig. 3(a), and the peak positions are consistent with those of metallic Rh. Approximately  $10 \text{ \AA}$  of the top surface was sputtered in the XPS chamber prior to analysis to remove adventitious surface oxygen and carbon. The measured Rh  $3d^{3/2}$  and  $3d^{5/2}$  peak positions at 312.5 and 307.7 eV (referenced to carbon at 285 eV measured before sputtering) have a peak ratio of 2:3, while no C  $1s$  and very

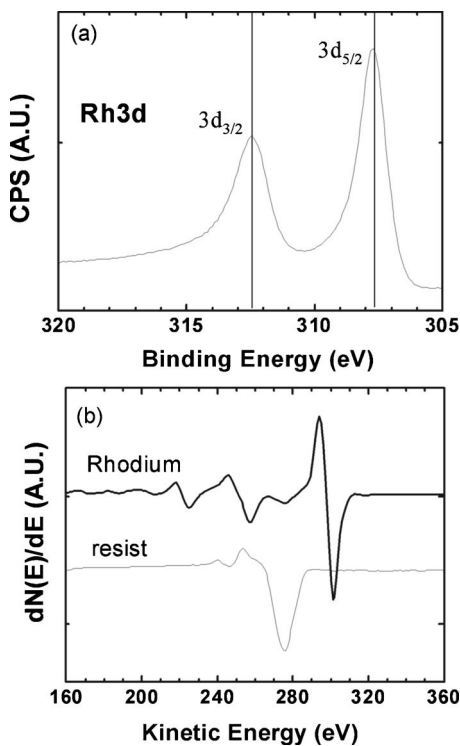


FIG. 3. (a) Rh  $3d$  XPS spectrum of an ALD rhodium film on  $\text{SiO}_2$ . (b) AES spectra showing selective area deposition of ALD Rh. The top spectrum is for Rh deposited on  $\text{SiO}_2$  at  $300^\circ \text{C}$  for 300 cycles using conditions described in text. The lower Auger spectrum (labeled "resist") is from the same sample, after exposure to 300 ALD cycles, collected from a region of sample covered by resist. The spectrum is consistent with carbon in the resist, with no rhodium on the resist surface within the sensitivity of the AES ( $\sim 0.5$  at. %).

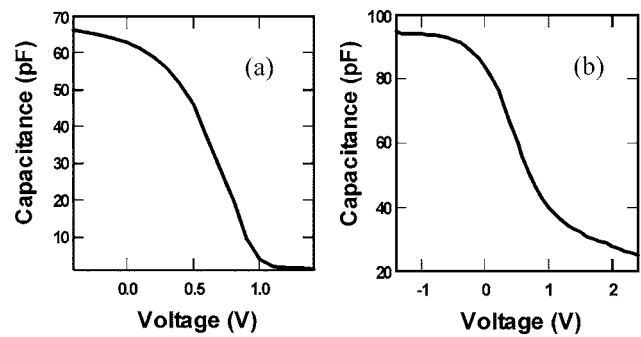


FIG. 4. Capacitance vs voltage behavior of selectively deposited ALD Rh MOS capacitors: (a) on CVD  $\text{HfO}_2$  and (b) on  $\text{SiO}_2$ . Results show typical metal-oxide-semiconductor behavior, and for the sample shown, the flatband voltages  $V_{\text{FB}}=0.72$  and  $0.18 \text{ V}$  and equivalent oxide thicknesses  $EOT=5.7$  and  $4.8 \text{ nm}$  for  $\text{HfO}_2$  and  $\text{SiO}_2$ , respectively.

small O  $1s$  peaks are observed. The oxygen sensitivity factor is small in XPS, making oxygen content difficult to quantify, but the peaks indicate an O atomic fraction of  $\sim 0.09$ . We believe further process optimization could reduce the oxygen content.

To achieve selective deposition,<sup>3,15</sup> photoresist ( $\sim 1 \mu\text{m}$ ) was first deposited on  $\text{SiO}_2$  and  $\text{HfO}_2$  and patterned, and then baked in air at  $100^\circ \text{C}$  for 5 min. Substrates with patterned resist were then transferred into the deposition chamber and heated at the deposition temperature for 15 min before deposition was initiated. After 300 cycles, deposition was visible on the oxide, with no visible deposition on the photoresist, consistent with inhibited Rh nucleation on the resist.<sup>3,5</sup> Figure 3(b) shows AES data from one sample exposed to 300 cycles of the Rh ALD process at  $300^\circ \text{C}$ . Data were collected from a region of the sample (AES probe area  $\sim 10^{-4} \text{ cm}^2$ ) originally not covered by resist (top spectrum) and a region covered by resist (bottom spectrum). The AES spectrum on the resist shows a distinct C  $KLL$  peak, with no evidence of the Rh  $MNN$  peak at 320 eV or satellite peaks between 200 and 280 eV. This demonstrates selectivity to Rh nucleation on the resist within the sensitivity of the AES ( $\sim 0.5$  at. %). We note that when hexamethyldisilazane (HMDS) was used as a resist adhesion promoter, nucleation was also inhibited on the oxide surface. Contact angle measurements suggest that some HMDS remains on the oxide surface after resist patterning, which likely impedes precursor adsorption.

A key benefit to selective area deposition is that it eliminated the need for Rh etching in device fabrication. Capacitors were formed by direct selective area ALD, and the CV behavior, shown in Figs. 4(a) and 4(b), was evaluated directly upon removal of the samples from the reactor system. To extract the effective work function of the gate electrode in the metal/oxide/semiconductor stack,<sup>16</sup> the flatband voltage ( $V_{\text{FB}}$ ) was estimated<sup>17</sup> for several capacitors with various equivalent oxide thicknesses (EOTs). Under conditions of minimal bulk dielectric charge, a plot of  $V_{\text{FB}}$  versus EOT is expected to follow the relation  $V_{\text{FB}}=\Phi_{\text{ms}}-(Q_f EOT)/\epsilon_{\text{ox}}$ , where the slope ( $Q_f$ ) is the fixed charge at the semiconductor/dielectric interface and the linear intercept ( $\Phi_{\text{ms}}$ ) is the metal/semiconductor work function difference. The value for the effective work function ( $\Phi_{\text{m,eff}}$ ) is found from the semiconductor work function ( $\Phi_s$ ) using  $\Phi_{\text{ms}}=\Phi_{\text{m,eff}}-\Phi_s$ . Plots of  $V_{\text{FB}}$  versus EOT are shown in Fig. 5,

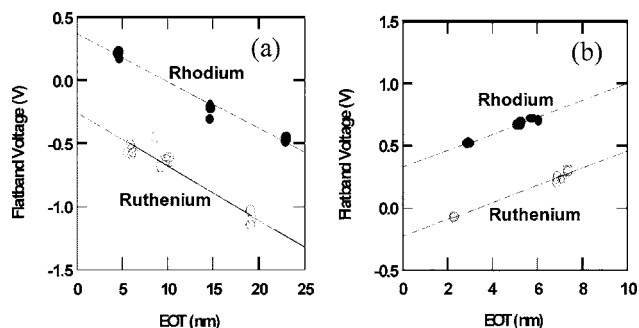


FIG. 5.  $V_{FB}$  vs EOT for (a) Rh/SiO<sub>2</sub>/Si and Ru/SiO<sub>2</sub>/Si and (b) Rh/HfO<sub>2</sub>/Si and Ru/HfSiO<sub>x</sub>/Si. *p*-type Si with doping levels of  $7 \times 10^{17}$  and  $3 \times 10^{15}$  cm<sup>-3</sup> was used for SiO<sub>2</sub> and HfO<sub>2</sub>, respectively. All fits show a quality (*R*) of  $\sim 0.9$ .

and the effective work functions of as-deposited ALD Rh on SiO<sub>2</sub> and HfO<sub>2</sub> were determined to be 5.43 and 5.25 eV, respectively. The slope of the fit gives a negative fixed charge density of  $1.5 \times 10^{12}$  cm<sup>-2</sup> at the Si/HfO<sub>2</sub> interface and a positive fixed charge density of  $8.1 \times 10^{11}$  cm<sup>-2</sup> at the Si/SiO<sub>2</sub> interface. Also included in Fig. 5 are results from CV analysis of ALD ruthenium films after reactive ion etch patterning and post-metal-anneal, deposited in the same reactor system using similar dielectric materials.<sup>3</sup> It is interesting to note that the as-deposited Rh capacitors have the same fixed charge as the Ru capacitors measured after post-metal-anneal. Thermal stability of Rh capacitors was also measured after forming gas anneal, and results showed a significant increase in EOT after anneal, consistent with oxidation of the semiconductor substrate.

Oxygen vacancies at the dielectric/metal interface created by annealing in reducing ambient can lead to a change in interface dipole and a net decrease in the apparent work function,<sup>8,9</sup> and subsequent annealing in an oxidizing ambient can return the work function to the previous values. In the ALD process reported here, some oxygen is present in the as-deposited Rh, likely resulting from residual oxygen used in the deposition process. This oxygen could be acting to passivate or impede vacancy creation in the as-deposited films, promoting the observed high work function values. The increase of EOT observed upon anneal is consistent with

excess oxygen diffusing from the Rh to oxidize the silicon substrate. It is important to note that the values of effective work function reported here for Rh in the as-deposited state are higher by  $\sim 100$ – $200$  meV than the highest values observed for other elemental PMOS gate metals such as Pt and Re.<sup>8</sup> Further studies related to controlling effective work function of Rh or other PMOS metal gate materials will require further process optimization, including detailed analysis of oxygen content, as well as vacancy creation and oxygen stability at the high-*k*/metal interface.

The authors gratefully acknowledge support from SEMATECH and the Semiconductor Research Corporation (SRC) under the Front End Processing Research Center.

- <sup>1</sup>S.-H. Lo, D. A. Buchanan, and Y. Taur, *IBM J. Res. Dev.* **43**, 327 (1999).
- <sup>2</sup>H. Kim, *J. Vac. Sci. Technol. B* **21**, 2231 (2003).
- <sup>3</sup>K. J. Park, J. M. Doub, T. Gougousi, and G. N. Parsons, *Appl. Phys. Lett.* **86**, 051903 (2005).
- <sup>4</sup>V. Misra, H. C. Zhong, and H. Lazar, *IEEE Electron Device Lett.* **23**, 354 (2002).
- <sup>5</sup>S. K. Dey, J. Goswami, D. F. Gu, H. de Waard, S. Marcus, and C. Werkhoven, *Appl. Phys. Lett.* **84**, 1606 (2004).
- <sup>6</sup>Y.-C. Yeo, T.-J. King, and C. Hu, *J. Appl. Phys.* **92**, 7266 (2002).
- <sup>7</sup>V. V. Afanas'ev, M. Houssa, A. Stesmans, and M. M. Heyns, *J. Appl. Phys.* **91**, 3079 (2002).
- <sup>8</sup>D. Lim, R. Haight, M. Copel, and E. Cartier, *Appl. Phys. Lett.* **87**, 072902 (2005).
- <sup>9</sup>J. K. Schaeffer, L. R. C. Fonseca, S. B. Samavedam, Y. Liang, P. J. Tobin, and B. E. White, *Appl. Phys. Lett.* **85**, 1826 (2004).
- <sup>10</sup>T. Aaltonen, M. Ritala, Y. L. Tung, Y. Chi, K. Arstila, K. Meinander, and M. Leskela, *J. Mater. Res.* **19**, 3353 (2004).
- <sup>11</sup>O. K. Kwon, J. H. Kim, H. S. Park, and S. W. Kang, *J. Electrochem. Soc.* **151**, G109 (2004).
- <sup>12</sup>T. Aaltonen, M. Ritala, and M. Leskela, *Electrochem. Solid-State Lett.* **8**, C99 (2005).
- <sup>13</sup>J. C. Hooker, T. Aaltonen, A. Rahtu, M. Ritala, M. Leskela, F. Roozeboom, E. Van den Heuvel, J. Van Zijl, M. Maas, and T. Raymakers, *Proceedings of the AVS Atomic Layer Deposition Conference 2004, Helsinki, Finland, 16–18 August 2004* (AVS, Chico, CA, 2004).
- <sup>14</sup>K. J. Park, S. M. Stewart, and G. N. Parsons (unpublished).
- <sup>15</sup>R. Chen, H. Kim, P. C. McIntyre, and S. F. Bent, *Appl. Phys. Lett.* **84**, 4017 (2004).
- <sup>16</sup>D. K. Schroeder, *Semiconductor Materials and Device Characterization* (Wiley, New York, 1990).
- <sup>17</sup>J. R. Hauser and K. Ahmed, in *Characterization and Metrology for ULSI Technology* edited by D. G. Seiler (AIP, New York, 1998), pp. 235–239.